

Robust Data Hiding Using Inverse Gradient Attention

Honglei Zhang^{*1}, Hu Wang^{*2}, Yuanzhouhan Cao¹, Chunhua Shen², Yidong Li^{†1}

¹School of Computer and Information Technology, Beijing Jiaotong University, Beijing, China

²The University of Adelaide, Australia

honglei.zhang@bjtu.edu.cn, hu.wang@adelaide.edu.au, yzhcao@bjtu.edu.cn, chunhua.shen@adelaide.edu.au, ydli@bjtu.edu.cn

Abstract

Data hiding is the procedure of encoding desired information into an image to resist potential noises while ensuring the embedded image has little perceptual perturbations from the original image. Recently, with the tremendous successes gained by deep neural networks in various fields, data hiding areas have attracted increasing number of attentions. The neglect of considering the pixel sensitivity within the cover image of deep neural methods will inevitably affect the model robustness for information hiding. Targeting at the problem, in this paper, we propose a novel deep data hiding scheme with Inverse Gradient Attention (IGA), combining the ideas of adversarial learning and attention mechanism to endow different sensitivity to different pixels. With the proposed component, the model can spotlight pixels with more robustness for embedding data. Empirically, extensive experiments show that the proposed model outperforms the state-of-the-art methods on two prevalent datasets under multiple settings. Besides, we further identify and discuss the connections between the proposed inverse gradient attention and high-frequency regions within images.

Introduction

Data hiding is to embed as much as general information (*e.g.*, messages) into a cover image without introducing too much perceptual difference from the original image. Meanwhile, the embedded message can be robustly reconstructed under some image distortions. There are three key factors to measure a data hiding model, *robustness*, *imperceptibility*, and *capacity* (Panchal and Srivastava 2015). The robustness refers to the reliability of message reconstruction even under any intentional image transformations. The imperceptibility refers to the similarity between the cover image and the encoded image, while the capacity refers to the amount of information that a model can embed into a cover image. So a robust data hiding system should satisfy the trade-off triangle relationships among them. Due to the effectiveness and security of data hiding, it has been widely used in digital watermarking (Kumar, Singh, and Yadav 2020) and steganography tasks (Zhang et al. 2021).

The general message embedded by a robust data hiding model can survive under various distortions, such as blur-



Figure 1: Visualization of some cover images from COCO dataset and their corresponding inverse gradient attention (IGA) masks. **Top:** The cover images. **Bottom:** The IGA masks visualized by transferring them into RGB domain.

ring, cropping, and JPEG compression. To achieve this goal, some traditional methods typically utilize heuristics to hide messages through texture (Bender et al. 1996) or frequency domain (Kundur and Hatzinakos 1998). For instance, the information can be embedded in the spatial domain by substituting the least significant bits (LSB) of the pixel values (Celik et al. 2005). In recent years, some deep learning based methods have achieved outstanding performance. HiDDeN (Zhu et al. 2018) applied the nature of generative adversarial network (GAN) and learned invisible perturbations to encode a rich amount of useful information. Similarly, Luo *et al.* used GAN as attacking network to generate agnostic image distortions to improve the model robustness (Luo et al. 2020).

Since in a cover image, different pixels have different importance to noises, some works explore the attention-based models for information hiding. Most recently, Yu *et al.* (Yu 2020) proposed to learn an attention mask through a CNN model to locate the inconspicuous areas of cover images, which are suitable for embedding messages. Nevertheless, the proposed neural attention model is black-box, and it introduces extra learnable parameters. Besides, they do not take the pixel sensitivity into account, which inevitably limits the robustness of models to encode complicated information. In this work, we propose to learn a novel attention mask, known as the Inverse Gradient Attention (IGA), obtained from the already existing gradients toward message reconstruction loss on the cover image pixels, which avoids introducing more trainable parameters. Moreover, our IGA

^{*}These authors contributed equally.

[†]Corresponding author.

scheme is more explainable compared with general attention-based models, because the gradients of pixels towards the message reconstruction objective generally show the sensitivity of pixels, which has been explored by (Goodfellow, Shlens, and Szegedy 2015). Thus, the inverse of gradients denote the robustness of pixels, which in turn indicate how much attention should be assigned to the corresponding pixels for message encoding.

The purpose of visualization in Fig. 1 is to give an intuition of the inverse gradient attention mask generated by our IGA model. The inverse gradient values locate the pixels that are robust for message embedding. Though this simple yet effective method, our proposed model improves the robustness of the data hiding model against various image distortions.

In summary, our main contributions are listed below:

- We propose to generate inverse gradient attention (IGA) scheme to perceive more robust pixels of cover images for data hiding. The IGA scheme helps our model to be more robust to resist a variety of image distortions.
- We conduct extensive experiments on two prevalent datasets and instantiate them on two canonical data hiding models. Empirically, our proposed model can surpass its counterparts by a large margin and achieve state-of-the-art performance.
- Moreover, we further identify and discuss the connections between the proposed inverse gradient attention with high-frequency regions within images.

Related Work

Follow the development vein of data hiding technology, we divide related work into two categories for clear explanation: traditional data hiding approaches and deep learning based data hiding approaches.

Traditional Data Hiding Approaches.

The traditional data hiding methods mainly adopt human heuristics to select pixels for information embedding. According to the domains of manipulating pixels, it can be further divided into spatial domain data hiding (Bamatraf, Ibrahim, and Salleh 2010; Pevný, Filler, and Bas 2010) and frequency domain data hiding (Lu et al. 2015; Parah et al. 2016; Bi et al. 2007). For the spatial domain paradigm, Tomas *et al.* (Pevný, Filler, and Bas 2010) proposed the HUGO algorithm to manipulate the least significant bits of certain pixels of the cover image. From the frequency domain perspective, some algorithms changed middle frequency components of the cover image in the frequency domain (Bi et al. 2007), and others exploited the correlation between Discrete Cosine Transform (DCT) coefficients of the adjacent blocks (Parah et al. 2016). Several reversible transforms like the Discrete Wavelet Transform (DWT) (Ganic and Eskicioglu 2004), or the Discrete Fourier Transform (DFT) (Tsui, Zhang, and Androutsos 2008) are also widely used to embed the watermarks in a robust and imperceptible way.

Deep Learning based Data Hiding Approaches.

Due to the remarkable representation ability of deep neural networks, an increasing number of powerful deep data hiding

models have been proposed (Baluja 2017; Yu 2020; Ahmadi et al. 2020; Luo et al. 2020; Ahmadi et al. 2020; Zhang et al. 2021). Specifically, HiDDeN (Zhu et al. 2018) utilized the adversarial learning mechanism and applied a single type of noise in a mini-batch and swapped it in each iteration to enhance the model robustness, which is a unified end-to-end framework for digital watermarking and steganography. Besides, Luo *et al.* (Luo et al. 2020) proposed distortion agnostic model to adversarially add noises by an attacking network to achieve the purpose of adaptive data augmentation, and applied channel coding to inject redundancy in the encoded message to improve the robustness of the watermarking model. Since different pixels have different importance to distortions in the cover image, ABDH (Yu 2020) adopted attention-based CNN model to perceive more inconspicuous pixels to improve the robustness.

Compared with the existing methods, one main difference of our model is that we embrace the joint ideas of adversarial learning and attention mechanism to generate an inverse gradient attention mask to effectively find robust pixels in the cover image in an end-to-end framework, instead of adding adversarial examples into the training set as data augmentation (Luo et al. 2020).

Proposed Method

Overall Architecture

We illustrate the overall architecture of our proposed method in Fig. 2. It consists of an inverse gradient attention module, a message coding module, an encoder and a decoder.

Inverse Gradient Attention Module. In our proposed model, we apply the inverse gradient attention (IGA) to enhance the model robustness. The IGA module generates an attention mask \mathbf{A} , which indicates the gradients of input cover image \mathbf{I}_{co} toward the message reconstruction loss. Intuitively, the gradient values generally show the robustness of each pixel for message reconstruction. In the next sub-section, we will introduce it in details.

Message Coding Module. The intuition behind this mechanism is that before embedding long message into the cover image, we can find a compact alternative representation, which will cause less disturbance on the premise of the same amount of information. As theoretically proved by (Hornik, Stinchcombe, and White 1989), any continuous mapping can be approximated by a neural network with one hidden layer. Based on this theory, we apply multi-layer perceptrons (MLPs) to map the original message from lengthy texture space into a compact encoded message space. Specifically, we adopt a symmetric structure for message coding, *i.g.*, a message encoder and a message decoder. The message encoder takes a binary message $\mathbf{M} \in \{0, 1\}^k$ of length k as input and outputs an encoded message $\mathbf{M}_{en} \in \mathbb{R}^l$ of length l , where $l < k$. Then at the end of our architecture, the message decoder is inputted $\mathbf{M}_{de} \in \mathbb{R}^l$ and outputs the recovered message $\mathbf{M}_{out} \in \{0, 1\}^k$. Note that our message coding is different from the channel coding proposed in (Luo et al. 2020). The channel coding is to produce a redundant message to enhance robustness, while our message coding is to reduce the dimension of the message to enhance the model capacity.

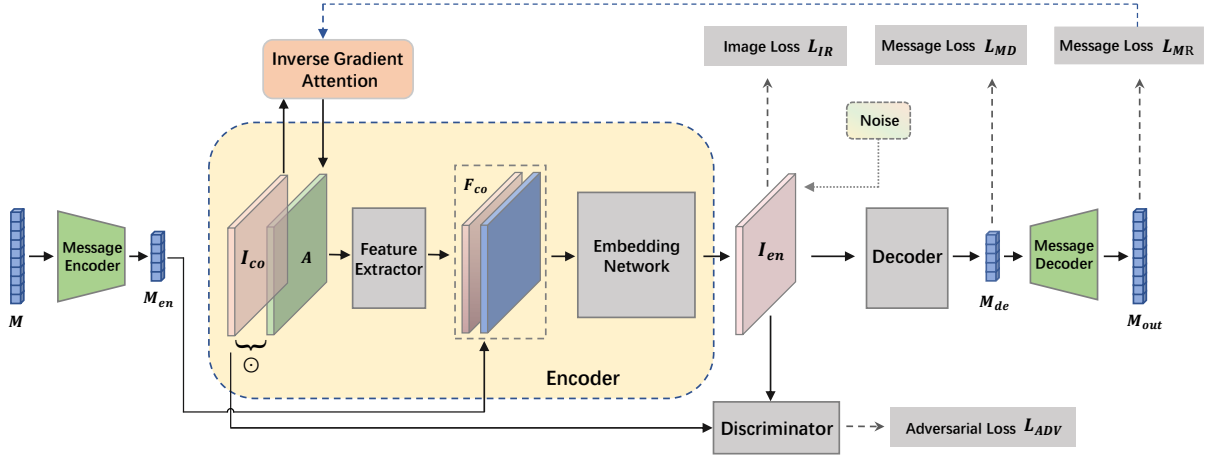


Figure 2: The framework of the proposed IGA model. The message to be embedded \mathbf{M} is fed into the Message Encoder to produce a compact representation \mathbf{M}_{en} . Meanwhile, the inverse gradient attention \mathbf{A} for the cover image \mathbf{I}_{co} is computed for the gradients towards the message reconstruction loss. Once the IGA mask \mathbf{A} is fetched, the Hadamard product of it and the cover image \mathbf{I}_{co} is required to obtain the attended image. Then, the attended image is fed into the Feature Extractor \mathcal{E} to produce intermediate feature maps \mathbf{F}_{co} . Later on, the \mathbf{F}_{co} and the encoded message \mathbf{M}_{en} are concatenated to generate the encoded image \mathbf{I}_{en} through the Embedding Network. Then, the Decoder Network produces a reconstructed decoded message \mathbf{M}_{de} . At last, the decoded message \mathbf{M}_{de} is further fed into the Message Decoder to produce the final recovered message \mathbf{M}_{out} .

Encoder and Decoder Module. After the attended image \mathbf{I}_{co}^A is fetched from cover image \mathbf{I}_{co} with the attention mask \mathbf{A} , the encoder takes the attended image \mathbf{I}_{co}^A and the encoded message \mathbf{M}_{en} as input and outputs an encoded image \mathbf{I}_{en} . The encoded image is then fed into the decoder to reconstruct the message \mathbf{M}_{de} . Finally the message decoder takes as input \mathbf{M}_{de} and outputs the recovered message \mathbf{M}_{out} .

Inverse Gradient Attention

For a data hiding model, the embedded message needs to be robustly reconstructed under image distortions. In order to achieve promising robustness, we need to locate the robust pixels for message reconstruction in the cover image, and then impose the message on these pixels. As described in FGSM (Goodfellow, Shlens, and Szegedy 2015), applying small but intentionally worst-case perturbations towards vulnerable pixels to the original image can result in outputting a totally incorrect result with high confidence. Inspired by this work, we propose a straightforward yet effective way to locate those robust pixels for message reconstruction. Specifically, the attention mask \mathbf{A} is generated by calculating the inverse normalized gradients of cover image \mathbf{I}_{co} toward the message reconstruction loss L_{MR} through back-propagation. Formally, this process can be presented as:

$$\mathbf{A} = \mathbf{T} - g(\nabla_{\mathbf{I}_{co}} L_{MR}(\mathbf{M}, \mathbf{M}_{out})), \quad (1)$$

where \mathbf{T} represents the tensor containing all ones. g denotes the general normalization function, *e.g.*, sigmoid or min-max normalization function, as the weights of the image pixels. We emphasize the differences between FGSM and our proposed IGA model here. Firstly, our model is not the generation of adversarial examples, so different norms are no

longer required. Besides, the tuning of ϵ adopted in (Goodfellow, Shlens, and Szegedy 2015) is not needed, since in IGA the soft and accurate inverse gradient attention is computed (between $[0, 1]$) rather than hard sign calculation.

Intuitively, the inverse gradient attention mask highlights the pixels that are robust for message reconstruction. In this case, we are able to encode messages robustly on these pixels. Particularly, we first obtain the Hadamard product of the cover image \mathbf{I}_{co} with the obtained attention mask \mathbf{A} . The multiplication is performed in a pixel-wise manner, the attended image \mathbf{I}_{co}^A is therefore obtained. Then, the attended image is fed into the feature extractor \mathcal{E} and the output is concatenated with the encoded message \mathbf{M}_{en} to formulate the input of embedding network \mathbf{F}_{co} :

$$\mathbf{F}_{co} = \mathcal{E}(\mathbf{A} \odot \mathbf{I}_{co}) \oplus \mathbf{M}_{en}, \quad (2)$$

where \mathbf{M}_{en} is generated by the message encoder in message coding module. \odot denotes the Hadamard product and \oplus represents the concatenation operation. The IGA training procedure iteratively conducts inverting of the original gradient-based attention tensor as the inverse attention mask, which forces the network to perceive their less sensitive pixels and in turn indicates how much weights should be assigned to the corresponding pixels, so as to achieve the purpose of embedding information robustly.

Loss Functions

We apply four loss functions to train our proposed model: two message loss functions to ensure the model robustness, an image reconstruction loss and an adversarial loss function to ensure the model imperceptibility. The MSE loss is adopted

for two message loss functions that are defined as:

$$L_{MR} = \lambda_{MR} \frac{1}{k} \sum_p (\mathbf{M}(p) - \mathbf{M}_{out}(p))^2, \quad (3)$$

and

$$L_{MD} = \lambda_{MD} \frac{1}{l} \sum_p (\mathbf{M}_{en}(p) - \mathbf{M}_{de}(p))^2, \quad (4)$$

where p denotes an element in message, and λ_{MR} and λ_{MD} represent the weight of message reconstruction loss and decoding loss, respectively. L_{MR} enforces the reconstructed message to be close to the original input, and L_{MD} enforces the decoded message to be close to the encoded message.

We also adopt MSE loss as our image reconstruction loss to enforce the encoded image to be close to the cover image:

$$L_{IR} = \lambda_I \frac{1}{N} \sum_{i,j} (\mathbf{I}_{co}(i,j) - \mathbf{I}_{en}(i,j))^2, \quad (5)$$

where i and j represent the pixel location and N is the total number of pixels. Besides, λ_I denotes the weight factor of the message reconstruction loss.

In order to further enforce the imperceptibility of our model, we apply the generative adversarial learning scheme by introducing a discriminator to increase the perception similarity between the encoded image and the original one (Goodfellow et al. 2014). Specifically, we treat the encoder as a generator to produce the encoded image with very similar to the cover image, and attempts to confuse the discriminator, while the discriminator is to recognize the encoded images from the original ones. The objective of our generative adversarial learning can be represented as:

$$L_{ADV} = \begin{cases} \max_D & \lambda_D \mathbb{E}_{\mathbf{x} \in \zeta} [\log(D(\mathbf{x})) + \log(1 - D(G(\mathbf{x})))], \\ \min_G & \lambda_G \mathbb{E}_{\mathbf{x} \in \zeta} [\log(1 - D(G(\mathbf{x})))] \end{cases}, \quad (6)$$

where \mathbf{x} is the input cover image and ζ represents its distributions, and G denotes the generator and D represents the discriminator. Besides, the variables λ_D and λ_G denote the weight factors of the maximization and minimization process respectively. When the whole process achieves Nash Equilibrium where the discriminator returns the classification probability 0.5 for each pair of encoded image and cover image (Goodfellow et al. 2014), the encoded image is almost completely indistinguishable from the original image so as to improve model imperceptibility.

Experiments

In this section, we introduce our experimental settings and present the extensive experimental results that validate the effectiveness of our model. Finally, we discuss the relationship between the proposed IGA and high-frequency image regions to offer more insights.

Experimental Settings

Datasets. To verify the effectiveness of our proposed model, we utilize two real-world datasets for model training and evaluation, namely the COCO dataset (Lin et al. 2014) and DIV2K dataset (Agustsson and Timofte 2017). For COCO dataset, 10,000 images are collected for training, and evaluation is performed on the other 1000 unseen images. For DIV2K dataset, we use 800 images for training and 100 images for evaluation. For each image, there is a corresponding message which is uniformly sampled with a fixed length k .

Evaluation Metrics. To thoroughly evaluate the performance of our model and compared models, we apply a series of evaluation metrics. For model robustness, the bit prediction accuracy is utilized to evaluate the ability of data hiding model to withstand image distortions. It is defined as the ratio of the correct prediction between the input message M_{in} and the corresponding position of the reconstructed message M_{out} . For imperceptibility, we adopt the peak signal-to-noise ratio (PSNR) for evaluation. In addition, we also visually evaluate the encoded images. For the model capacity, we apply the Reed-Solomon bits-per-pixel (RS-BPP) (Zhang et al. 2019) as the metric which represents the average number of bits that can be reliably transmitted in an image.

Compared Models. To evaluate the effectiveness of our framework in multiple settings, we compare several canonical data hiding models. The brief introductions are listed below:

- HiDDeN (Zhu et al. 2018) is a unified end-to-end CNN model for digital watermarking and steganography.
- SteganoGAN (Zhang et al. 2019) introduces residual learning into steganography and can embed messages with different channel depths as well.
- DA (Luo et al. 2020) can resist unknown image distortions by adaptively adding noises through adversarial learning.
- ABDH (Yu 2020) proposes to learn an attention mask through a CNN model to locate the inconspicuous areas of cover images for embedding messages.

Implementation Details. In our implementation, images are resized to 128×128 for HiDDeN, DA and ABDH models, while for SteganoGAN model, images are resized to 400×400 . To keep a fair comparison, we adopt the exactly same settings with compared methods, *i.g.*, 128×128 for IGA, and 400×400 for IGA*¹. We apply *Combined Noises* (CN) mechanism to train all models, where the model randomly select one particular kind of noise from the noise set $\{Crop, Cropout, Resize, Dropout, Jpeg\ compression\}$ at each time for a mini-batch of training, so as to improve the robustness of the model resisting complex noises. At the validation period, we utilize the well-trained model to test on a single noise respectively to verify the robustness of the model against various distortions.

We emphasize here that the parameters of the compared models completely experiment with the settings of the corresponding papers claimed for fair comparison. For our IGA model, the weight factors λ_{MR} , λ_{MD} , λ_I , λ_D and λ_G are

¹Note that we equip the proposed two components on SteganoGAN and make corresponding adjustments to our model for multiple-channel message embedding to keep a fair comparison.

Table 1: Comparison results on the COCO and DIV2K datasets. All models are trained and evaluated with various message lengths and image distortions. We adopt 3 message lengths $k = 30, 64, 90$, and 6 image distortions. *Identity* refers to no distortion.

Methods	COCO								DIV2K						
	k	<i>Identity</i>	<i>Crop</i>	<i>Cropout</i>	<i>Dropout</i>	<i>Resize</i>	<i>Jpeg</i>	<i>CN</i>	<i>Identity</i>	<i>Crop</i>	<i>Cropout</i>	<i>Dropout</i>	<i>Resize</i>	<i>Jpeg</i>	<i>CN</i>
HiDDeN	30	98.10	80.34	75.96	76.89	82.72	84.09	76.30	73.72	68.24	60.92	63.78	66.28	66.37	58.05
	64	79.82	72.52	63.20	68.53	69.35	68.85	65.46	70.45	51.60	51.09	52.40	50.81	50.99	52.35
	90	77.56	65.46	60.20	61.49	63.03	63.21	62.07	68.04	50.63	51.50	50.22	51.40	51.16	51.84
ABDH	30	98.70	85.16	74.82	75.31	80.23	82.62	74.01	81.09	62.24	59.71	58.72	60.83	63.44	63.58
	64	85.93	67.14	59.96	62.62	62.02	61.74	59.14	64.58	51.69	52.21	53.32	55.20	52.72	50.78
	90	75.22	52.65	51.99	52.88	52.95	53.04	52.25	66.44	51.48	51.67	51.28	51.15	51.19	50.23
DA	30	99.50	81.15	78.58	77.13	81.72	82.83	75.73	78.80	77.32	77.11	74.55	71.01	82.35	63.85
	64	77.18	68.68	65.82	73.00	62.54	73.58	64.90	62.01	62.65	61.79	71.09	58.91	71.26	53.31
	90	70.82	63.51	61.08	64.28	62.62	67.00	63.21	57.88	58.12	54.18	57.32	55.68	62.17	53.05
IGA (Ours)	30	99.96	86.88	79.33	77.51	81.44	87.35	80.30	79.94	77.39	60.93	76.63	72.19	82.90	64.14
	64	94.34	73.34	66.82	70.23	69.41	72.07	68.38	77.61	63.11	62.00	70.14	59.64	72.31	57.03
	90	84.62	69.45	62.52	64.96	65.78	68.78	64.32	71.50	59.10	55.31	60.10	56.48	63.21	57.14

Table 2: Comparison results with the SteganoGAN model on the COCO and DIV2K datasets.

Methods	COCO			DIV2K	
	D	<i>Identity</i>	<i>CN</i>	<i>Identity</i>	<i>CN</i>
SG	1	97.91	62.38	98.29	61.38
	2	96.02	62.63	96.53	58.11
	3	86.19	56.64	89.10	55.86
	4	76.10	53.39	78.07	53.03
	5	70.98	53.41	71.31	52.65
IGA* (Ours)	1	99.67	68.70	99.39	67.65
	2	99.07	65.04	98.62	58.65
	3	95.26	59.05	95.64	57.92
	4	84.56	55.78	84.28	57.46
	5	77.78	55.02	77.97	56.59

set 1.0, 0.001, 0.7, 1.0 and 0.001, respectively, for COCO and DIV2K datasets. In the training phase, the Adam optimizer (Kingma and Ba 2015) with default hyperparameters is adopted. The batch size is set to 32. For the proposed IGA model, the Feature Extractor Network, Embedding Network, Decoder Network and Discriminator Network are all composed of multiple convolution layers. For our message coding module, unless otherwise claimed, we set the encoded message length $l = 30$ for evaluation.

Quantitative Analysis on Robustness

In this section, we evaluate the model robustness through the bit prediction accuracy and compare with other data hiding methods. We conduct the experiments on the COCO and DIV2K datasets. Since in the HiDDeN, DA and ABDH models, the embedded message is one-dimensional binary string $\mathbf{M} \in \{0, 1\}^k$, we compare our method with these three methods and illustrate the results in Table 1. As for the SteganoGAN model, the embedded message is a binary tensor $\mathbf{M} \in \{0, 1\}^{D \times H \times W}$, we compare our method with the SteganoGAN model and illustrate the results in Table 2.

Table 1 gives a comprehensive comparison with the com-

Table 3: Quantitative comparison of encoded image quality varying different message channels on two datasets. The larger the PSNR values, the better the encoded image. Besides, the first place of each column is bolded and the symbol ‘_’ represents the same performance as the compared model.

Methods	COCO			DIV2K	
	D	<i>Identity</i>	<i>CN</i>	<i>Identity</i>	<i>CN</i>
SG	1	27.10	30.10	39.03	43.01
	2	26.43	31.87	37.56	46.02
	3	27.16	32.21	36.98	46.02
	4	27.21	31.7	38.23	46.02
	5	26.88	30.8	40	46.02
IGA* (Ours)	1	31.40	32.80	43.01	<u>43.01</u>
	2	31.10	32.04	40	<u>46.02</u>
	3	30.45	32.40	46	<u>46.02</u>
	4	30.96	32.40	38	<u>46.02</u>
	5	30.83	32.59	<u>40</u>	<u>46.02</u>

pared models across various message lengths and image distortions. We can see from the results that our method outperforms the three methods in the majority of settings. When the message length is 30 or 64, only under a few image distortions that our results are slightly lower than the compared models. And when the message length is 90, our results are significantly better under all distortions. This shows that our method can embed rich information robustly. It’s worth mentioning that our model is consistently superior to the ABDH model under most settings, which reflects that our attention mechanism generated by inverse gradient is more effective than the black-box attention methods.

Table 2 shows the comparison results of our model with the SteganoGAN model. From the results, we can see that our method achieves the best performance with different number of message embedding channels under various noises on both datasets. Moreover, it is worth mentioning that our method has better accuracy with message channel $D = 5$ than the SteganoGAN model with message channel $D = 4$

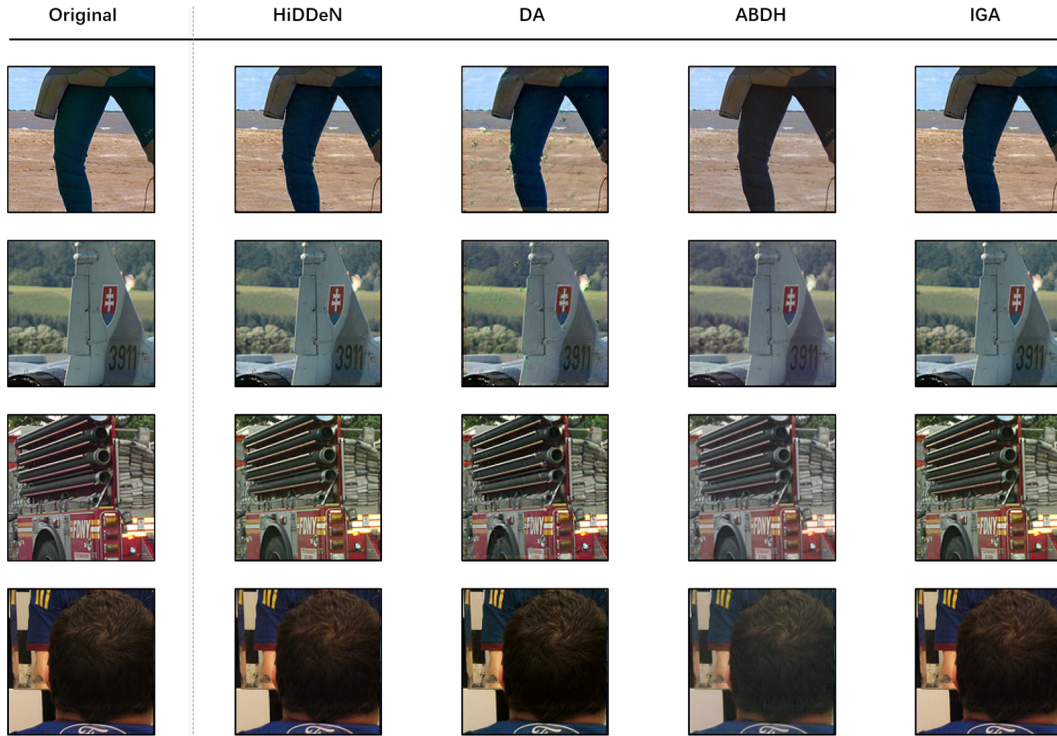


Figure 3: Multiple samples of original and encoded images from COCO dataset. The first column presents the original images. The remaining columns depict the visualization of the embedded images of the compared models and the proposed IGA model.

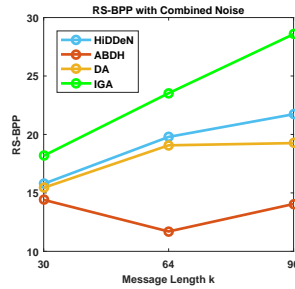
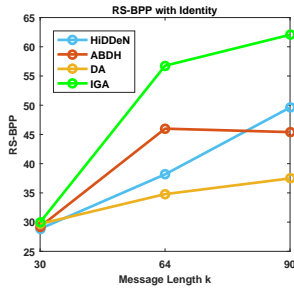


Figure 4: Capacity comparison with compared models on COCO dataset under Identity and Combined Noises settings.

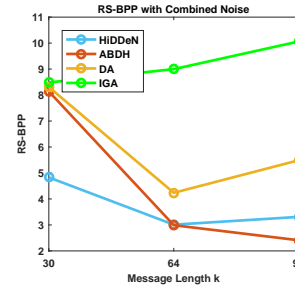
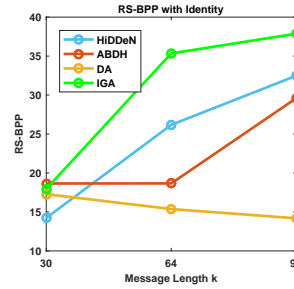


Figure 5: Capacity comparison with compared models on DIV2K dataset under Identity and Combined Noises settings.

on the COCO dataset and achieves comparable results on the DIV2K dataset. This indicates that our method can embed more information than other models when the accuracy is similar. It also reflects the proposed IGA model plays a positive role to improve model capacity.

Qualitative Analysis on Imperceptibility and Capacity

Besides the model robustness, the quality of embedded image is also critical for data hiding. We conducted the experiments about the quantitative comparisons of imperceptibility with the settings of *Combined Noises* and the message length $k = 30$, and the results are comparable with other canonical

data hiding models. Fig. 3 presents the visualization results of the proposed IGA model and the counterparts. The figure generally shows our method can not only have exceptional robustness, but also take the imperceptibility of the embedded image into account. It can be observed that the encoded images generated by our method and the compared methods are visually similar, as well as with cover images. In addition, the PSNR comparison of the proposed IGA model with the SteganoGAN model is provided in Table 3. From the table, our method achieves the best performance in both *Identity* and *Combined Noises* settings on the COCO dataset. Moreover, the performance of our method is comparable in most cases on the DIV2K dataset. This experiment proves that our

Table 4: Ablation study results on COCO and DIV2K datasets with multiple settings.

Methods	COCO		DIV2K	
	<i>Identity</i>	<i>CN</i>	<i>Identity</i>	<i>CN</i>
<i>Basic</i>	77.56	62.07	71.04	50.73
<i>w MC.</i>	78.12	62.93	71.21	51.67
<i>w Att.</i>	84.47	65.88	71.47	55.59
<i>Both</i>	84.62	64.32	71.50	57.14

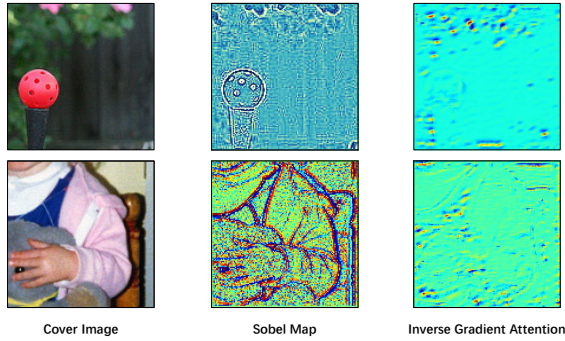


Figure 6: The cover image and its corresponding sobel heatmap and inverse gradient attention heatmap.

method is more robust under the premise of imperceptibility.

To measure the capacity of data hiding models, Fig. 4 and Fig. 5 present the RS-BPP results of our model compared with other methods on both COCO and DIV2K datasets. We can observe that the capacity of the model gradually increases with the length increasing of the embedded message. Moreover, the performance of our method is better than the compared methods, whether it is under the case of *Identity* or *Combined Noises* settings. In light of this observation, our proposed algorithm is verified to improve the model capacity significantly for more message embedding.

Ablation Study

In this section, we evaluate the contribution of the message coding module and the inverse gradient attention mask in our proposed method and show the results in Table 4. We conduct experiments on both the COCO and DIV2K datasets. For the *Basic* model, it's based on the pure Encoder-Decoder framework with generative adversarial loss, and the *Both* model is on the basis of the *Basic* model equipped with our inverse gradient attention and message coding module. Besides, the *w Att.* model is with our inverse gradient attention module, and the *w MC.* is equipped with the message coding module and the message decoding loss. From Table 4 we can see that both the message coding module and the inverse gradient attention mask make positive impacts on the performance. And the performance improvement mainly comes from the inverse gradient attention mask. Message encoding is a accessory module, but it shows the effectiveness under most circumstances. In one case, the message coding module

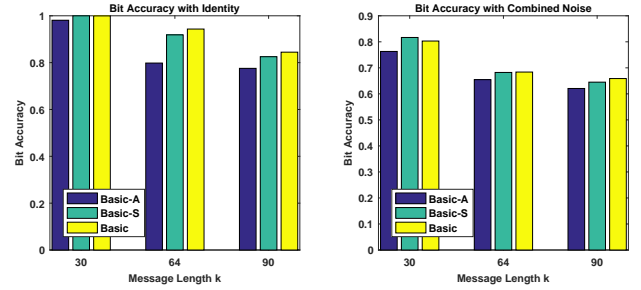


Figure 7: Performance comparison with the inverse gradient attention and the Sobel operator on COCO dataset. Among them, Basic-S represents the algorithm using Sobel edge operator, and Basic-A represents our algorithm with inverse gradient attention mask to perform data hiding task.

is slightly worse under the CN criteria. We hypothesis the random combined noises complicate the features in the high dimensional space incurring difficulties to learn under this circumstance.

Discussion

In this work, we use the Sobel operation as the high-frequency area extractor since it is very efficient to stand out edge regions in an image, which are the high-frequency areas in the image frequency domain. Through the visualization of the inverse gradient attention mask, we perceive that the inverse gradient attention mask is activated strongly in some edge regions, *e.g.*, the map acquired from Sobel operation. Fig. 6 shows the corresponding Sobel Map and Inverse Gradient Attention over cover images. Some similarities between sobel map and inverse gradient attention can be observed.

According to the observation, we further conduct experiments by substituting the IGA mask with the Sobel map for our data hiding framework. The comparative experimental results on COCO datasets are shown in the Fig. 7. It can be seen that by adopting the Sobel map for data hiding, the model also achieves promising performance. The experimental result empirically shows attending pixels with rapidly changing frequency (*i.e.*, edge regions) generally has a similar effect as inverse gradient attention for model robustness enhancement. It is further discovered that the proposed IGA model receives better results on all cases than the model with Sobel map, since the proposed IGA mechanism is able to attend pixels adaptively toward robust message hiding. It also indicates that not all edge regions are suitable for information hiding.

Conclusion

In the paper, we propose a novel end-to-end deep data hiding model with Inverse Gradient Attention (IGA) mechanism allowing the model to mine more robust pixels for data hiding. Moreover, we further identify and discuss the connections between the proposed inverse gradient attention with high-frequency regions within images. From extensive experimental results, our proposed IGA model is able to achieve superior performance than current state-of-the-art methods.

References

- Agustsson, E.; and Timofte, R. 2017. NTIRE 2017 Challenge on Single Image Super-Resolution: Dataset and Study. In *CVPR Workshop*, 1122–1131.
- Ahmadi, M.; Norouzi, A.; Karimi, N.; Samavi, S.; and Emami, A. 2020. ReDMark: Framework for residual diffusion watermarking based on deep networks. *Expert Syst. Appl.*, 146: 113157.
- Baluja, S. 2017. Hiding Images in Plain Sight: Deep Steganography. In *NeurIPS*, 2069–2079.
- Bamatraf, A.; Ibrahim, R.; and Salleh, M. N. B. M. 2010. Digital watermarking algorithm using LSB. In *ICCAIE*, 155–159.
- Bender, W.; Gruhl, D.; Morimoto, N.; and Lu, A. 1996. Techniques for data hiding. *IBM Sys. Jour.*, 35(3.4): 313–336.
- Bi, N.; Sun, Q.; Huang, D.; Yang, Z.; and Huang, J. 2007. Robust Image Watermarking Based on Multiband Wavelets and Empirical Mode Decomposition. *IEEE Trans. Image Process.*, 16(8): 1956–1966.
- Celik, M.; Sharma, G.; Tekalp, A.; and Saber, E. 2005. Lossless generalized-LSB data embedding. *IEEE Trans. Image Process.*, 14: 253–266.
- Ganic, E.; and Eskicioglu, A. M. 2004. Robust DWT-SVD Domain Image Watermarking: Embedding Data in All Frequencies. In *MM&SEC*, 166–174.
- Goodfellow, I.; Pouget-Abadie, J.; Mirza, M.; Xu, B.; Warde-Farley, D.; Ozair, S.; Courville, A.; and Bengio, Y. 2014. Generative Adversarial Nets. In *NeurIPS*, 2672–2680.
- Goodfellow, I. J.; Shlens, J.; and Szegedy, C. 2015. Explaining and Harnessing Adversarial Examples. In *ICLR*.
- Hornik, K.; Stinchcombe, M.; and White, H. 1989. Multilayer feedforward networks are universal approximators. *Neural Networks*, 2: 359–366.
- Kingma, D. P.; and Ba, J. 2015. Adam: A Method for Stochastic Optimization. In *ICLR*.
- Kumar, S.; Singh, B. K.; and Yadav, M. 2020. A Recent Survey on Multimedia and Database Watermarking. *Multim. Tools Appl.*, 79(27-28): 20149–20197.
- Kundur, D.; and Hatzinakos, D. 1998. Digital watermarking using multiresolution wavelet decomposition. In *ICASSP*, 2969–2972.
- Lin, T.; Maire, M.; Belongie, S. J.; Hays, J.; Perona, P.; Ramanan, D.; Dollár, P.; and Zitnick, C. L. 2014. Microsoft COCO: Common Objects in Context. In *ECCV*, 740–755.
- Lu, J.; Wang, M.; Dai, J.; Huang, Q.; Li, L.; and Chang, C. 2015. Multiple Watermark Scheme based on DWT-DCT Quantization for Medical Images. *J. Inf. Hiding Multim. Signal Process.*, 6(3): 458–472.
- Luo, X.; Zhan, R.; Chang, H.; Yang, F.; and Milanfar, P. 2020. Distortion Agnostic Deep Watermarking. In *CVPR*, 13545–13554.
- Panchal, U. H.; and Srivastava, R. 2015. A Comprehensive Survey on Digital Image Watermarking Techniques. In *CSNT*, 591–595.
- Parah, S. A.; Sheikh, J. A.; Loan, N. A.; and Bhat, G. M. 2016. Robust and blind watermarking technique in DCT domain using inter-block coefficient differencing. *Digit. Signal Process.*, 53: 11–24.
- Pevný, T.; Filler, T.; and Bas, P. 2010. Using High-Dimensional Image Models to Perform Highly Undetectable Steganography. In *Information Hiding*, 161–177.
- Tsui, T. K.; Zhang, X.-P.; and Androustos, D. 2008. Color Image Watermarking Using Multidimensional Fourier Transforms. *IEEE Trans. Inf. Forensics Secur.*, 3: 16–28.
- Yu, C. 2020. Attention Based Data Hiding with Generative Adversarial Networks. In *AAAI*, 1120–1128.
- Zhang, C.; Lin, C.; Benz, P.; Chen, K.; Zhang, W.; and Kweon, I. S. 2021. A Brief Survey on Deep Learning Based Data Hiding, Steganography and Watermarking. *arXiv preprint arXiv:2103.01607*.
- Zhang, K. A.; Cuesta-Infante, A.; Xu, L.; and Veeramachaneni, K. 2019. SteganoGAN: High Capacity Image Steganography with GANs. *arXiv preprint arXiv:2001.09678*.
- Zhu, J.; Kaplan, R.; Johnson, J.; and Fei-Fei, L. 2018. HiD-DeN: Hiding Data With Deep Networks. In *ECCV*, 682–697.